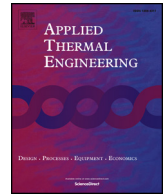




ELSEVIER

Contents lists available at ScienceDirect

Applied Thermal Engineering

journal homepage: www.elsevier.com/locate/apthermeng

Performance assessment of seawater cooled chillers to mitigate urban heat island



Luigi Schibuola, Chiara Tambani*

University IUAV of Venice, Dorsoduro 2206, 30123 Venice, Italy

HIGHLIGHTS

- The effect on UHI of the heat released to urban canyon by chillers was investigated.
- The case study of a coastal city was studied by an archetype modeling approach.
- Urban Weather Generator model and dynamic simulations provided the performances.
- Sea water cooled chillers linked to an urban grid is the mitigation strategy proposed.
- Results highlight clear energy and environmental benefits vs air cooled chillers.

ARTICLE INFO

Keywords:

Urban heat island
Seawater cooled chillers
Resilient city
Urban weather model
Anthropogenic heat
District cooling network

ABSTRACT

Urban heat island (UHI) phenomenon, nowadays accentuated by global warming, is growing its negative influence on urban resilience, building energy budget and human comfort during summer. To reduce UHI effect, mitigation strategies are normally focused on actions related to urban design like the use of high reflectivity surfaces and increase of vegetation. But, as concerns building anthropogenic heat, the benefits of a possible reduction of the heat released by air conditioning systems to neighborhoods are often underestimate. An effective solution consists in transporting the heat emitted by chiller condensers elsewhere by using water as heat transfer fluid. The systematic use of seawater to cool chillers in an urban area of a coastal city was investigated. The modification of the UHI phenomenon was studied as well as the consequences on building cooling demands and chiller performances assessed in dynamic conditions. Urban weather files in presence of different types of chillers were elaborated by Urban Weather Generator model. Building cooling demands in the area were evaluated by using archetype modeling approach and EnergyPlus model. The algorithm adopted to assess chiller performances takes into account also the effect of part load working condition. The comparison of seawater cooled chillers technology versus the more diffuse use of air cooled chillers highlights a significant UHI effect reduction which reaches 57% during the night. As regards cooling demand increment caused by UHI, with seawater cooled chillers it is reduced of 58%. In the end, thanks to lower demand and higher chiller efficiency, seawater cooling chillers achieve an energy saving of 23.5%. Therefore this solution can foster the urban resilience and sustainability with an increasing contribution in front of the future climate scenario. Therefore, the introduction of a district cooling network is an important UHI mitigation strategy and its feasibility would have to be always verified between the possible actions.

1. Introduction

Global warming and climate changes are a relevant concern for environment and human activities and, at the same time, a new challenge for 21st century cities, projected in a scenario of environmental strong fragility system. Nowadays, it is widely recognized by the international scientific community, in particular by the

Intergovernmental Panel on Climate Changes (IPCC), that the crucial and invasive contribution of anthropogenic activity overlaid the environmental systems cyclical natural changes [1]. Resilience is cities ability to react to these changes and this concept interprets a new and more pragmatic concept of sustainability [2]. Considering how much importance climatic variable is acquiring in the current scenario of changes, cities are the main place to test urban systems adaptability.

* Corresponding author.

E-mail address: chiara.tambani@iuav.it (C. Tambani).

<https://doi.org/10.1016/j.applthermaleng.2020.115390>

Received 19 February 2020; Received in revised form 14 April 2020; Accepted 22 April 2020

Available online 28 April 2020

1359-4311/ © 2020 Elsevier Ltd. All rights reserved.

For this reason interest in increasingly resilient cities is growing. Indeed, a combination of factors like cities fast growth and climate changes favors urban thermal stress and poses critical challenges to urban environments, underlining the need to investigate resilience measures to mitigate high urban temperatures [3,4].

The widest known urban climate phenomenon is the urban heat island (UHI) effect. It is characterized by higher temperatures in urban areas than in their rural or less urbanized neighborhoods. Comprehensive reviews [5,6] clearly show this phenomenon for various cities worldwide. Beside human comfort deterioration, urban temperatures increment worsens building air conditioning strengthening the cooling demand and consequent electricity absorption peak and reducing air-conditioners efficiency [7,8]. Simultaneously, high urban temperatures considerably decrease cooling potential techniques like natural and night ventilation [9]. About pollution UHI influences are conflicting. On one hand UHI increases electric consumption for air conditioning and consequently air pollutants and greenhouse gas emissions from power stations. In addition higher temperatures can directly foster the ground-level ozone formation [10,11]. On the other hand UHI temperatures can contribute to reduce particulate matter concentration thanks to major air turbulence induced [12,13].

This thermal increment has its origin from different causes: 1) urban built surfaces, mainly composed of low solar radiation reflectance and high heat storage capacity materials such as concrete and asphalt [14] in comparison with green infrastructures which instead deflect solar radiation and reduce heat storage by releasing moisture into the atmosphere; 2) different height and size buildings that generate urban canopies hindering the infrared emission to sky; 3) urban canyon reducing the wind effect [15]; 4) anthropogenic heat generated directly in the street or inside buildings [16]. As concerns the first three UHI mechanisms, effective countermeasures are proposed by exploiting suitable building geometry and surface materials with high albedo [17,18], as well as a systematic increment of urban green areas [19–21]. Anthropogenic heat is emitted especially during daytime, largely due to human activity, traffic and building air conditioning and in some cases it can be considered as the driving force of the entire phenomenon [22,23]. While urban landscape transformation affects outside air temperature by altering the radiative and convective heat fluxes from urban surfaces over time, the anthropogenic heat represents a direct heat gain immediately supplied to urban environment. Energy consumption wastes heat to environment affecting, indeed, intensity and spatial-temporal variability of urban climate [24,25]. For this reason, action plans to reduce UHI effect have to consider also procedures to reduce energy consumption starting from a better understanding of correlations between environmental effects and energy systems behavior [26,27]. This need moves researchers specialized in energy and environment to expand their interest to urban field, trying to incorporate UHI effects into thermal simulations [28]. Various dynamic calculation programs have been widely used to simulate buildings energy performances, adopting as climate data the so-called 'typical meteorological year' (TMY) or easily achievable real records from rural or airport stations, as inputs for use in simulations. However, these meteorological records fail if used for the altered climatic conditions within urban contexts, which are highly affected by local and site-specific factors, such as surface structures, land cover and human activity. Consequently, the use of rural climate data for the energy simulation of urban buildings may lead to inaccurate prediction of energy demands. In previous studies, two methods were used to assess UHI impact on buildings energy use. The first one is the straightforward approach using in situ meteorological observations as input for building energy simulation (BES) tools [29,30]. The second one is the modeling approach, which uses modeled climatic data to assess energy impact of UHI [31,32]. One result of modeling approach is the so called Urban Weather Generator (UWG) tool [33], a type of software that couples urban scale evaluations with a building simulation model, based on EnergyPlus [34]. This way, EnergyPlus calculations can include the

effects of other buildings sited in the surroundings. Among the numerous parameters used, UWG considers the anthropogenic heat generation. Previous studies show that it is one of the most sensitives [35]. In this context, the application of ground water to eliminate the anthropogenic heat quota connected to air conditioning can provide significant advantages. Nowadays the use of geothermal energy as heat source/sink for heat pumps has met great interest owing to the less seasonal temperature variations with respect to the air source [36]. Different technologies can be developed on the basis of the use of groundwater from wells, surface water (lake, river, sea) or directly ground coupled by an heat exchanger [37]. A systematic installation of ground heat exchangers in existing urban areas is less feasible. Water usually permits marked advantages like a low installation cost and no surface area required. In addition ground heat exchangers can release heat also in the first ground layers directly under the urban area with possible increment of subsurface UHI in summer [38]. Surface water can be a valid alternative for the buildings sited in proximity of significant surface water bodies like rivers, lakes or seas [39–42] and particularly tempting in coastal cities. In fact, in open sea context, the presence of sea currents helps a quick removal from the coast in front of the urban area of the released heat and the mixing of water with different temperature levels reducing water heating effect if compared to less extended superficial aquifers (ponds, lagoons). In air conditioning applications the energy advantages have been clearly highlighted [43]. These promising results have stimulated studies about economical and energy optimization concerning large-scale application of seawater source heat pump in district heating and cooling [44,45]. In order to get reliable assessments of the performance under the widely variable boundary conditions taking place during the cooling season, building energy simulation tool here used includes validated calculation procedures aimed at the prediction of the chiller performance under part load conditions. In fact chillers are sized for peak load, so they usually run under part load conditions, far from the full load taken as reference.

This paper deals with the problem of the heat released to urban environment by HVAC systems. The consequence on UHI was evaluated and a solution to reduce this effect is proposed and analyzed in a case study. In detail the performance of surface water to reduce UHI is assessed by considering a systematic use of water cooled chillers instead of air cooled chillers (ACC) in order to avoid the release of heat from refrigeration machines directly in the urban canyon. As the case study is a coastal city, the use of seawater cooled chillers (SWCC) was considered here. The application of this technology was studied in a precise area of the city analyzed and its effects were investigated not only in terms of urban temperature reduction but also of energy and environmental possible benefits.

2. Method

2.1. Application to a case study

Jesolo is a seaside resort town on the Adriatic Sea near Venice city in Veneto region. The city's economy is mostly based on summer tourism with 15-Kilometre beach. In fact with around six million tourist presences per year (over 5.7 millions in the investigated year 2017), Jesolo is one of the largest beach resorts in Italy. The city grew intensely in the Post-War period as result of the strong increment of mass tourism. In particular, starting from the 1950s, this coastal area was affected by a sudden building speculation because there was still no regulatory plan that only twenty years later would have partially regulated the construction. A constructive saturation took place along the entire seafront with a ribbon-type settlement focusing more on the quantity than on the quality of the result. In this way, green areas, public gardens and collective equipment were sacrificed to leave space for the building. A regulatory plan, which became operational in 1977, and subsequently a complete masterplan drawn up in 1997 (by architect Kenzo Tange) finally put the city development in order according to

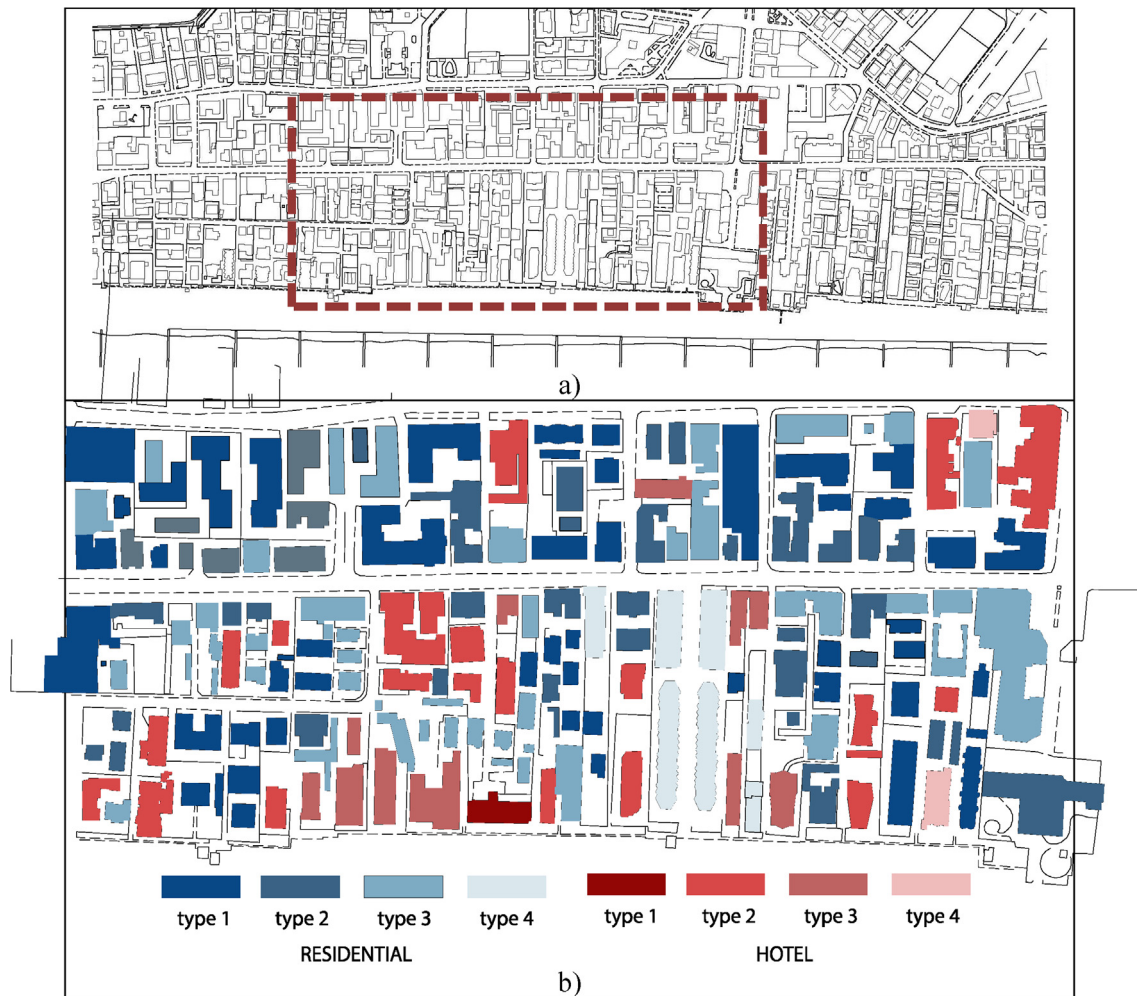


Fig. 1. Collocation of the investigated area in the urban fabric (a), detail of the area with the different building types marked (b).

modern criteria. The area studied in this work is located right in the area that developed between the 50s and 70s and retains the characteristics of this period. The selection is linked to the decision to deal with a critical area from the point of view of the environmental impact precisely because of the urban choices. The area is presented in Fig. 1a which shows the appearance of a portion of the urban belt overlooking the beach on the lower side and above by a road parallel to the sea. Fig. 1b shows urban density in detail and highlights a road parallel to the sea that cuts the area. This road is not particularly busy in daytime while it becomes a pedestrian zone between 8 pm and 6 am and in this way the most important promenade in the city saturated by shops, restaurants and bars normally located at the first floor of residential buildings. Numerous hotels are also present. The investigated area is about a rectangle with dimensions 620×262 m (total area 162440 m^2). Total built surface in percentage referred to total area is 36.7% and the building density referred to total area is $4.27 \text{ m}^3/\text{m}^2$. The total volume subdivided in the existing building typologies is reported in the Tables 1 and 2. As the tourism season is concentrated between the beginning of June and mid-September, this is the period studied.

The buildings normally retain the same characteristics of the construction period. As the first national law imposing thermal insulation in building was published in 1976, the envelopes of the buildings in the area are without insulation and through the years only the modification of the windows from single glazing to double glazing was normally carried on. This is also because these buildings are used only in summer and therefore heating is not foreseen. Instead air conditioning is present





practically in the totality of the buildings. Air cooled refrigeration machines are systematically used for this aim They consist of typical commercial products like split-systems or compact units as described in section 2.6.

2.2. Meteorological data used

The weather conditions used throughout the simulations pertained to actual weather data monitored during 2017. These data were received from the regional environmental agency ARPAV (Agenzia Regionale per la Prevenzione e Protezione Ambientale del Veneto) and collected by a meteorological station installed in rural area near the city of Jesolo and therefore not influenced by urban effects. For this reason the corresponding weather file is here named rural weather file. From the rural weather data the corresponding EnergyPlus weather file (EPW) was prepared, according to [46].

Especially during the touristic season, ARPAV monitors with continuity the environmental parameters of coastal seawater in front of the beaches. It provided us also the seawater temperature recorded at deep of 2 m near the investigated area. Fig. 2 shows the trends of rural outdoor and seawater temperatures in the summer 2017. As regards seawater temperature, the peak was $29.2 \text{ }^\circ\text{C}$ on July 21th and only in the period between 16 July and 15 August it exceeds $27 \text{ }^\circ\text{C}$. In Fig. 2 the trend of wind speed and monthly averages of the daily global solar radiation on horizontal surface are also reported. This location is not particularly windy and the solar radiations recorded in the period are typical for this area.





Table 1
Characteristics and simulation parameters of the hotel archetypes.

	Hotel archetypes			
	Type 1	Type 2	Type 3	Type 4
				
Period ^a	1930–1950	1950–1960	1960–1975	1960–1975
Floors ^a	4–5	3–7	4–8	9–18
Rooms ^a	40–80	14–48	50–99	100–160
Windows (% floor area) ^a	12.5–20	12.5–20	20–30	20–30
Number of buildings ^a	1	21	10	2
Total volume (m ³) ^a	6793	105,919	83,790	9375
Reference Surface (m ²) ^b	2264	1412	2244	6415
Reference volume (m ³) ^b	6793	3959	7860	22,502
Persons (n) ^b	165	90	180	470
Internal heat gain (W/m ²) ^b	6			
Cooling set point temp. (°C)	26			
HVAC schedule (h) ^b	0–24			
Air change rate (ACH) ^b	1			
Walls U-value (W/m ² K) ^b	1.41	0.81	0.98	1.22
Windows U-value (W/m ² K) ^b	3.2			
Windows SHGC (–) ^b	0.7			
Roof U-value (W/m ² K) ^b	1.61	1.44	1.33	1.89

^a Referred to all the buildings in the area.

^b Referred to each simulated archetype.

Table 2
Characteristics and simulation parameters of the residential archetypes.

	Residential archetypes			
	Type 1	Type 2	Type 3	Type 4
				
Period	1950–1970			
Floors	4–5	3	4–5	6–9
Commercial ground floor	No	Yes	Yes	Yes
Windows (% of floor area)(floorearea)	12.5–20	12.5–20	12.5–20	12.5–20
Number of buildings ^a	48	37	39	7
Total volume (m ³) ^a	119,450	67,263	209,639	91,250
Reference Surface (m ²) ^b	952	633	1731	5635
Reference volume (m ³) ^b	2570	1899	5194	16,905
Occupancy (W/m ²)	0.06	0.06 ^c or 0.1 ^d		
Internal heat gain (W/m ²)	4	4 ^c or 10 ^d		
Cooling set point temp. (°C)	26			
HVAC schedule (h)	12 pm–06 am	12 pm–06 am ^c or 9 am–12 m ^d		
Air change rate (ACH)	0.5	0.5 ^c and 1 ^d		
Walls U-value (W/m ² K)	0.82	1.41	0.87	1.22
Windows U-value (W/m ² K)	3.2			
Windows SHGC (–)	0.7			
Roof U-value (W/m ² K)	1.54	1.61	1.99	2.05

^a Referred to all the buildings in the area.

^b Referred to each simulated archetype.

^c Dwellings.

^d Commercial areas.

2.3. Urban area modeling

GIS data which contains usage, building coverage and height of individual buildings was utilized to model the area.

The modelling of building energy demand at urban scale is based on

the archetype modelling approach [47]. The total building stock of the area is subdivided in building categories according to the characteristics determining energy demand. For each building category an archetype building is selected to be used for building energy performance simulation. EnergyPlus code, a comprehensive and robust building

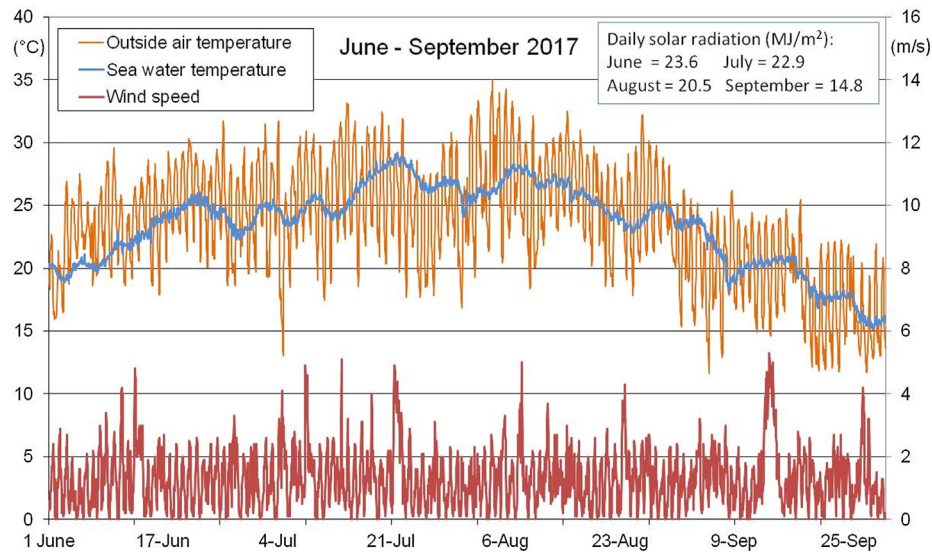


Fig. 2. Outside air temperature vs. seawater temperature in the period June-September 2017. Wind speed trend and monthly average daily global solar radiation on horizontal surface are also reported in the figure.

simulation engine, was chosen for this aim. The model is based on the contemporary solution of the global energy balance of each thermal zone of the building taking into account the contribution of HVAC system [29]. In detail the application of EnergyPlus provides the hourly profile of the cooling load of the archetype. This demand is divided for the building volume in order to estimate a cooling demand intensity which is adopted for all the buildings of each category. In this way the entire cooling requirement of the total building stock in the area is calculated by adding up the requirements referred to each building categories obtained multiplying the demand intensity for the total volume of the buildings of each category. The archetypes selected in this case study are reported in Table 1 for the hotels and in Table 2 for residential buildings. They were chosen to characterize the entire building stock of the area on the base of different geometry, size, envelope thermal characteristics, operation hours and internal usage. A significant part of the residential buildings presents commercial activities on ground floor (bars, restaurants and especially shops). In this case, similar internal parameters were assumed in Table 2 as more specific aspects like the presence of internal dining or coffee rooms is normally substituted by outdoor areas like courtyards and stallages without influences on the cooling load. Similarly kitchens are not served by air conditioning.

HVAC system configuration of the hotel archetypes adopts as indoor air conditioning unit Constant Air Volume (CAV) systems in the larger rooms (hall, dining and bar rooms) and fan coil units in the other rooms and in particular in the bed rooms. HVAC systems in the considered residential archetypes adopts fan coil units. Owing to the actual spreading of LED, lighting electric consumption is low and therefore not considered alone but included in the internal heat gain which considered also the consumption of the appliances. In the simulation typical schedule for occupant presence was adopted and used also as internal gain schedule.

As an example of the simulation outcomes, hourly profiles of the cooling load in a week of August for the archetypes hotel type 3 and residential type 3 are reported in Fig. 3a. In this case the simulations used rural weather file. Characteristics of the seasonal cooling demand of the area calculated by the archetype modelling approach are reported in Fig. 3b and c. Fig. 3b shows the percentage subdivision in the fourth summer months of the total seasonal demand simulated between the June 1th and September 15th. July and August are clearly the most important periods. September is almost negligible. In Fig. 3c the subdivision in percentage is referred to the usage of the air conditioned

volumes. Cooling demand quota of hotels and dwellings in the analysed area are similar and sharply greater than the contribution of the commercial facilities.

2.4. UWG code application

UWG model modifies a rural weather file and its output is an urban weather file taking into account UHI effects. To generate this urban weather file, UWG needs a parametric modelling of the city or district. In detail, UWG code calculates the hourly values of the mean air temperature inside an urban area starting from a rural meteorological file in EPW format and using an auxiliary file in XML format which describes the investigated area [48,49].

This description is based on a list of parameters necessary to model the UHI. In particular these informations are organized in four categories: urban morphology, vegetation characteristics, reference site data and buildings. The general values calculated for the investigated area are reported in Table 3. For the buildings, thermal properties of the envelope components of the archetypes were introduced. In particular a typical albedo value 0.2 is used. As regards the other informations about buildings the values of Tables 1 and 2 were used. For each HVAC system, UWG requires a chiller efficiency EER defined as reported in Table 5. Typical values were assumed and in detail 3.5 in the case of ACCs, 4.5 for SWCCs [50] These values were confirmed by the final outcomes. Another important parameter to be introduced in UWG is “heat released to canyon” which can give a value between 0 and 1. It represents the quota of wasted heat from cooling system that is exhausted into the urban area. Value 1 is typical for ACCs when the whole heat from condenser is released to the outside air in the canyon. Value 0 means that waste heat is not released into the canyon This is the case of SWCCs. Therefore two urban EPW file were obtained from UWG by these two possibility of “heat released to canyon” parameter. The first EPW named UHI_1 was obtained with the value 1 and the second EPW named UHI_2 with the value 0.

2.5. Description of the seawater cooling system

The proposal consists in the substitution of the existing ACCs with centralized water-to-water chillers, one for each building, cooled by a two pipes water network built in the analysed area. In detail, each chiller takes the water flow rate needed to cool its condenser from the delivery pipe of the grid by a dedicated pump and gives back it to the

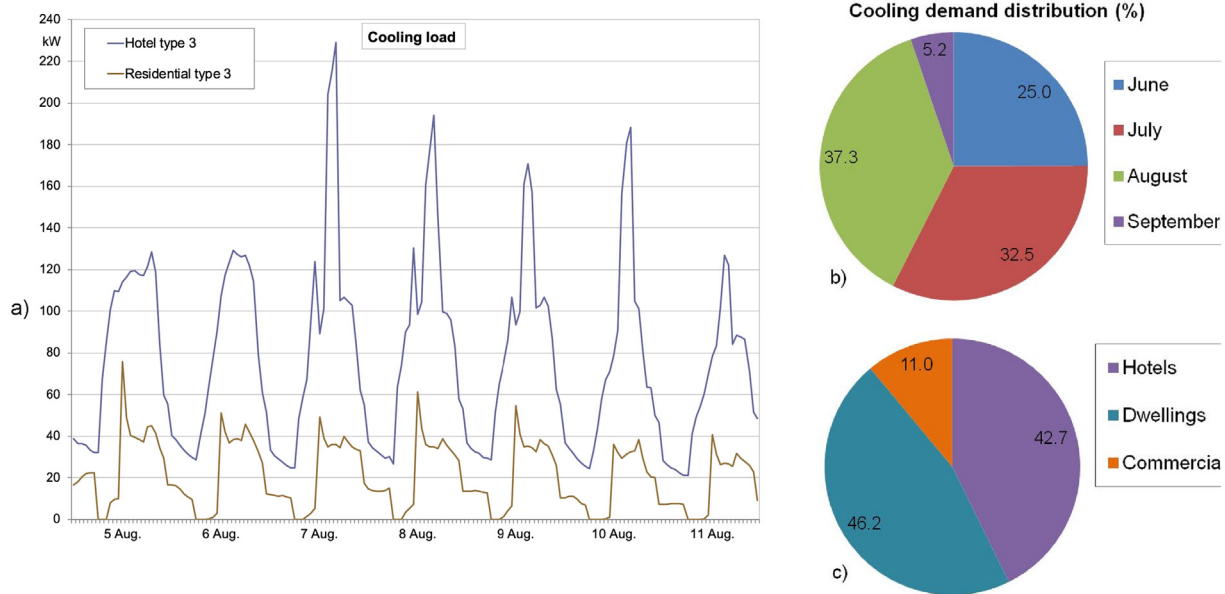


Fig. 3. . Cooling loads simulated with the rural weather: trends of hotel 3 and residential type 3 in a week of August (a), distribution of the total cooling demand of the area in the summer months (b) and with respect to the building usage (c).

Table 3
UWG model main parameters.

Urban area			
Average building height (m)	15.2	Vegetation albedo (-)	0.25
Site Coverage ratio (-)	0.367	Vegetation start/end (month)	1/12
Facade to site ratio (-)	1.17	Daytime boundary layer height (m)	700
Tree Coverage (-)	0.1	Nighttime boundary layer height (m)	80
Non building sensible heat (W/m ²)	7	Reference height	140
Non building latent heat (W/m ²)	0	Road albedo (-)	0.165
Char length (m)	228	Road emissivity (-)	0.95
Tree latent (-)	0.7	Vegetation Coverage (-)	0.01
Grass latent (-)	0.6	Material	Asphalt
Reference site			
Latitude (°)	45.5	Temperature measurement height (m)	10
Longitude (°)	12.5	Wind measurement height (m)	10

Table 4
Main data of the district cooling network and a scheme of the seawater cooling system.

Maximum simultaneous cooling demand of the condensers required from the network (kW)	14,874
Maximum water flow rate of the cooling closed network (m ³ /h)	2558
Maximum tube sizes Di/De (mm) and maximum length of single closed loop circuit (m)	515/630–1190
Maximum seawater flow rate (m ³ /h)	4263
Tube sizes Di/De (mm) and length of the seawater circuit (m)	705/800–210
Peak electric absorption of the pumping system (kW)	278 kW

return pipe. The water grid forms a closed loop linked to a technical station located near the seaside. Here a plate heat exchanger is interposed between the circuit sampling seawater and the cooling closed loop in order to avoid the fouling of the condensers inside the chillers. The current national legislation [51] prevents a thermal use of seawater which causes a change of temperature above 3 °C and also the outlet water temperature cannot exceed 35 °C. The heat exchanger is sized according to the worst condition permitted, i.e. a maximum

temperature difference for seawater of 32–35 °C which corresponds to a nominal water temperature drop 35–40 °C in the condenser side circuit. The water network of the area was designed on the basis of the simulation of the building loads and chiller performances described later in section 3.2 and using urban weather obtained by UWG in the case of SWCC. PE pipes buried underground are considered for this network. Network main data and a functional diagram of the seawater cooling system are reported in Table 4.

Pumping system is based on three pumps for the closed loop of the district network and the same for the seawater open circuit where the return to the sea is at 50 m from the suction point to avoid interferences. To reduce the electric absorption of the pumping system the control is fundamental. In presence of very frequent part loads, a reduced number of pumps can work alternatively. In addition a variable flow rate of the pumping is obtained by speed control of the pump electric motors via inverter technology. In order to follow the effective cooling demand the water flow rate control keeps constant the temperature difference between the return and supply water. This difference is 5 °C for the urban network and 3 °C for seawater open loop. This pumping control is very important. In fact in this way the calculated saving about electric consumption of pumping reaches the 83% in comparison with the case of constant flow rate. Normally in this kind of technical stations, two heat exchangers working alternatively for maintenance need are foreseen as well as a filter for seawater. However if a self-cleaning filter is adopted by intermittent reverse cycles of the water flows, the experience [52] has shown low level of fouling found in the heat exchangers. This fact indicates the possibility of using only one heat exchanger limiting the cleaning of the exchanger only in the end of summer period.

2.6. Chiller model

Both ACC and SWCC are provided with multiple scroll compressors, two stainless steel plate heat exchangers as evaporator and condenser and R410A brine. In ACC the condenser is an air cooled coil. Each analyzed archetype presents only one chiller. In hotels 1 and 2 the chiller has two fully hermetic rotary scroll compressors installed in only one refrigerant circuit. In hotel 3 and 4 both the chillers have two refrigerant circuits with two compressors each. The residential archetypes also present central systems of cold production with similar chillers and

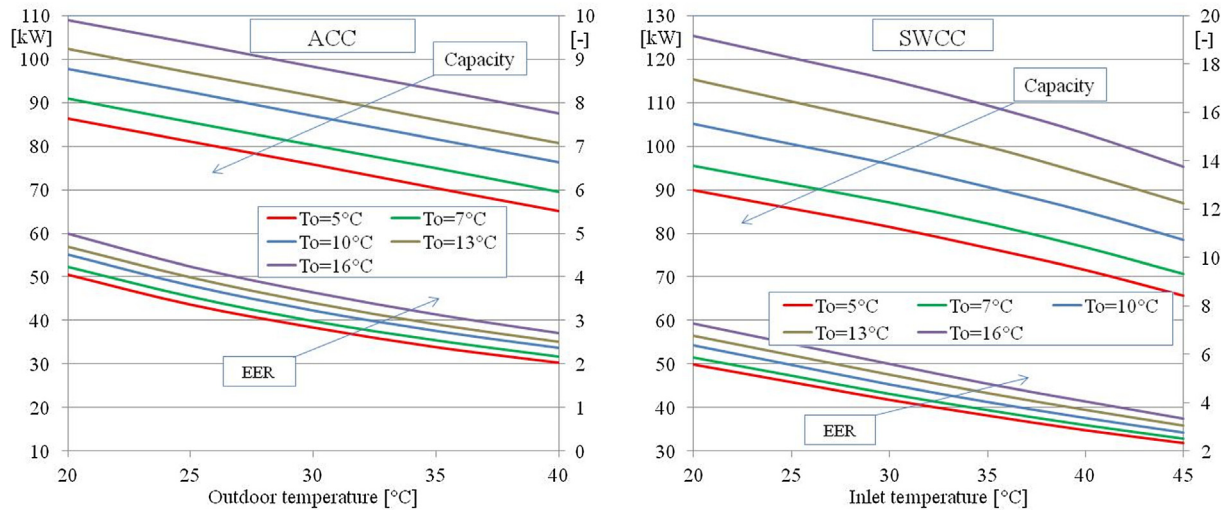


Fig. 4. Hotel 2: full load performances of the chillers as functions of inlet temperature at the condenser for SWCC or outdoor temperature for ACC and of outlet temperature T_o at the evaporator.

secondary systems based on fan coil units. Indeed especially in dwellings the outdated technology to use individual cooling by air-to-air split systems is still frequent, instead fan coil units are more diffuse in tertiary buildings. However the recent development of new models of fan coil units characterized by small dimensions and less sound emission is facilitating their diffusion also in residential buildings. In any case for the new SWCC central system for cold production (with individual energy accounting) is the best solution. For this reason it was assumed more correct for the comparison between SWCC and ACC to consider centralized cold production in both the cases without introducing for ACC further penalization connected with individual cooling technology. Evaporative towers to cool chillers are instead practically inexistent in Jesolo. However, their use is not the solution, since it only shifts thermal load from sensible to latent increasing outside relative humidity fundamental to determine human comfort.

Fig. 4 shows the full load performance of ACC and SWCC for hotel 2, in terms of efficiency and capacity rating for different thermal levels of the entering water temperatures at the evaporator and condenser (outdoor air temperature for ACC). The efficiency indexes are defined as summarized in Table 5. These data come from the manufacturer [53]. They were obtained as required by standard test methods [54]. The only difference in the components of the two chillers is the condenser. For SWCC a plate heat exchanger where inlet water is pumped by the district network. For ACC a coil cooled by outside air moved by a fan installed in the machine. For this reason in Fig. 4 the EER of SWCC

does not considered pumping electric consumption instead fan electric consumption is already taken into account in EER calculation of ACC. Pumping consumption is considered later. In the considered chillers the capacity control of each refrigerant circuit is based on tandem compressors with two stages, 50% and 100% of the total capacity. The manufacturer also provided the performance data at part load conditions required for the calculation of the European Seasonal Energy Efficiency Ratio ESEER [55]. These data are the four values required for the assessment of the Energy Efficiency Ratio (EER) respectively at 25, 50, 75 and 100% of full load capacity and obtained by laboratory tests.

The ESEER is a weighted average of these four values. Starting from these values, it is also possible to calculate the corresponding correction factor of the EER at full load, called Part Load Factor (PLF), which takes into account the effects of the part load operation to adjust the performance at full load [56].

In Fig. 5a, the trend of PLF is reported as a function of the Capacity Ratio (CR), which is the ratio of the actual capacity, equal to the load to be met, on the maximum capacity that the machine is able to provide at the same levels of operating temperatures. This curve is obtained by interpolation between the four previous values, while under 25% it was calculated with the simplified algorithm proposed by EN 14,825 [57] and reported in Eq. 5. Even if not coming up to the benefits allowed by modulating control of the capacity by inverter, Fig. 5a shows how the use of tandem compressors installed in the same refrigerant circuit enables better performance than full load, that is PLF greater than one, in a wide range of CR. This result is mainly due to the over-sizing of evaporator and condenser in part load operation rather than in full load. For this chiller modeling, a quasi-steady state calculation procedure based on a spreadsheet style model was used. At every time step, on the basis of actual values the full load performance curves (Fig. 4) give output capacity and efficiency EER as a function of the simultaneous measured values of the outdoor temperature and of the temperature of the cold water produced. The evaluation was made on the basis of the hourly averages of the measured data. The actual efficiency is obtained by multiplying the efficiency at full load by the PLF calculated according to CR (Fig. 5a). The electric consumption results from the ratio of the output capacity on the simultaneous efficiency. The monthly average EER is the ratio of the cooling energy supplied in a month on the monthly electric consumption. The annual average value is calculated analogously. A flow-chart of the modeling procedure is presented in Fig. 5b.

Table 5
Definitions of chiller efficiency and related terms.

$EER = \frac{P_c}{P_{el}}$	Eq. 1
$EER = EER_{fl} \cdot PLF(CR)$	Eq. 2
with	
$CR = \frac{P_c}{P_{c,fl}}$	Eq. 3
$PLF(CR) = \frac{EER}{EER_{fl}}$	Eq. 4
$PLF(CR) = \frac{CR}{C_c \cdot CR + (1 - C_c)}$	Eq. 5
where:	
	EER is the Energy Efficiency Ratio [-]
	P_c is the cooling capacity [kW]
	P_{el} is the electric power [kW]
	CR is the capacity ratio [-]
	PLF is the part load factor [-]
	fl refers to full load conditions
	C_c decay factor (0.9 as default value) [-]

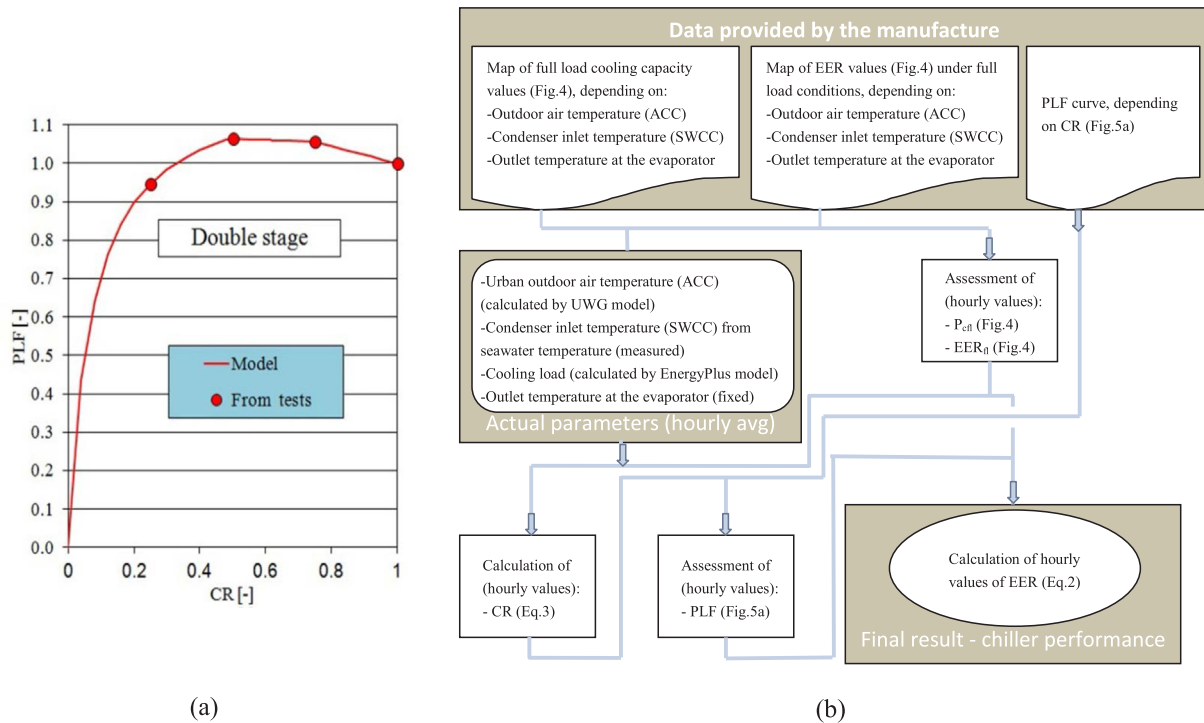


Fig. 5. Part Load Factor (PLF) as a function of the Capacity Ratio (CR) for each refrigeration circuit equipped with two compressors (double stage for the capacity control) (a) and flow chart for the calculation of chiller performance (b).

3. Results

3.1. UHI evaluation

First outcomings concern the differences in the temperature trends of the outdoor air in the cases of rural weather file monitored and urban weather calculated by UWG when ACCs (UWG_1) or SWCCs (UWG_2) are considered. Fig. 6 shows a comparison of the temperature trends for three days for each summer month and their average values for all day long, daytime and night are also reported. A net difference by using the three weather files is evident. In each hour the UHI effect is confirmed to be the same i.e. the UHI_1 temperature is the greatest and UHI_2 is between the other two temperatures. Environmental thermal condition becomes worst owing to building air conditioning. In Fig. 6 the corresponding UHI intensities and the contemporary wind speeds are also reported. UHI intensity is the difference between urban and rural temperature in the same moment. The UHI intensity is effectively reduced by introduction of SWCCs instead of ACCs. The comparison of UHI intensity vs. wind speed often indicates a clear influence of wind in reducing UHI effect

In Fig. 7a Total, daytime and night average air temperatures in the three cases are reported for each month and for the whole summer as well as the percentage differences of these temperatures. Fig. 7b shows the corresponding UHI intensities.

At seasonal level, in daytime the UHI_1 effect causes an average increment of 3.2% of the rural air temperature while UHI_2 only of 2.0%. The corresponding temperature difference between UHI_1 and UHI_2 is 1.2%. It means that the SWCC technology reduces the urban increment of 37% with respect to ACC during daytime. It is also noticeable that during the night the UHI effect is always greater than during daytime. In fact the night average increment with UHI_1 is 5.8% and 2.5% with UHI_2 and the temperature difference is 3.3%. Therefore the advantage of SWCC technology is confirmed with a UHI effect reduction of 57% during night. Similarly, the mean UHI intensities reported in Fig. 7b indicate a greater mitigation during night by using SWCC owing to the higher UHI intensity with respect to daytime.

3.2. Energy and environmental effects assessment

For all the buildings of each single archetype considered in the urban area modelling, Fig. 8a shows the comparison of the seasonal cooling requirements simulated by using the three different weather files. The corresponding percentage differences are also reported. Strong variations in cooling demand highlight consistent differences in the contribution of each archetype owing to their dimensions and numbers present in the area. However the UHI phenomenon has a clear influence to increase the cooling demand of all the building archetypes. But the percentage increment trends are quite different for the hotels and residential buildings. With UHI_1 conditions the residential cooling demand is more sensitive to UHI effect than hotels. This is probably because of the air conditioning schedule which excludes the morning and then it is concentrated in the remaining part of the day when the UHI phenomenon is more remarked (especially night). SWCC technology attenuates this characteristic thanks to the less temperature increment. In Fig. 8b the total cooling demand of the whole analysed urban area is presented for each month and referred to the seasonal period for the three different weather conditions. From the 8.86 GWh with rural weather condition, the seasonal demand increases up to 10.0 GWh with UHI_1 weather and 9.36 GWh with UHI_2. Therefore, the seasonal increment due to UHI_1 with respect to rural weather is 12.9% while with UHI_2 is only 5.7% and the percentage reduction of UHI_2 with respect to UHI_1 is 6.3%.

The percentage reduction of the demand increment thanks to UHI_2 is consequently equal to 55.8%. As regards monthly distribution, the quota relative to September is modest, but the UHI effects remain quite regular. The results confirmed that the building simulation in urban area must be carried on with weather file considering UHI phenomenon even if SWCC technology is able to reduce strongly the increment of the simulated demand in the previous evenience.

Fig. 9a shows monthly and seasonal average EER referred to all the chillers present in the analysed area with SWCC or ACC technology and the consequent primary energy savings obtained with SWCCs instead of ACCs. The effect of electric absorption of pumping is also considered for

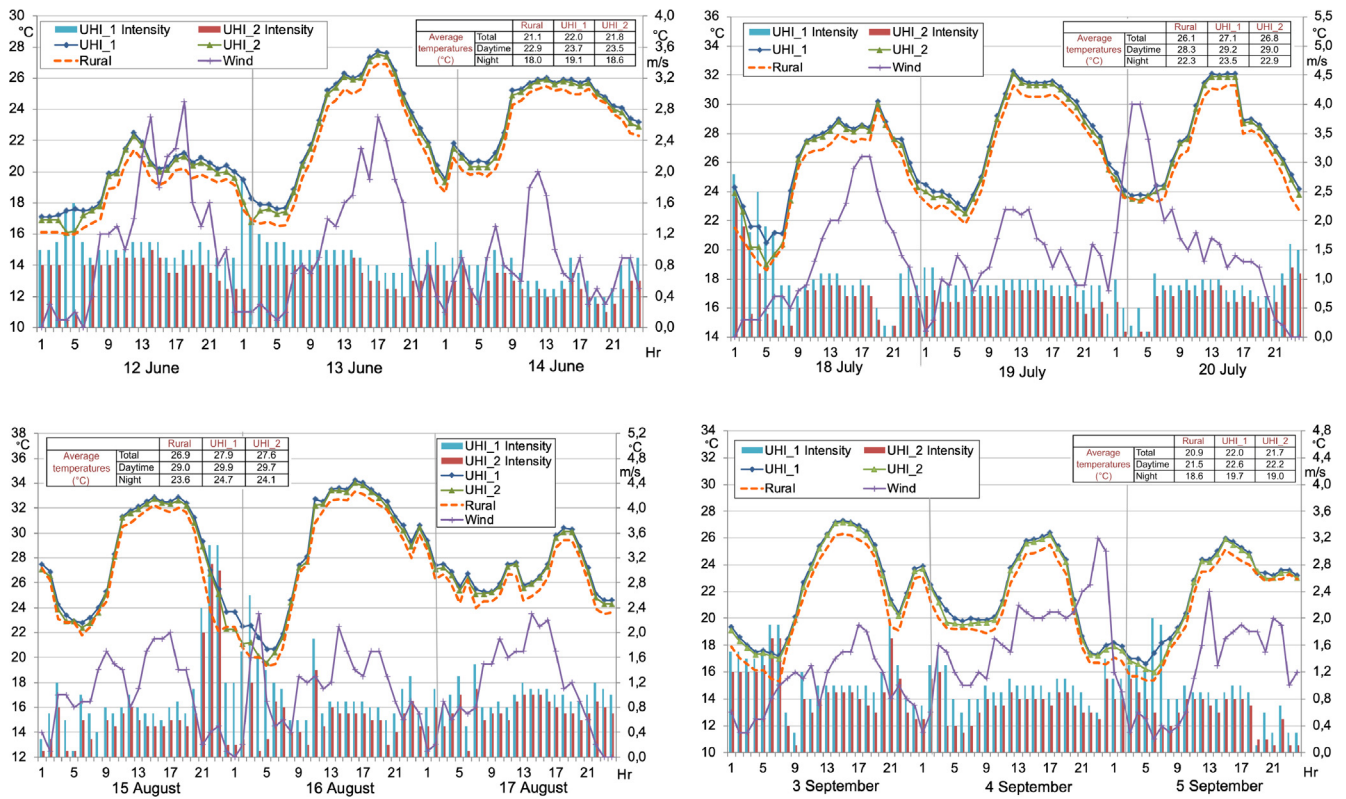


Fig. 6. Comparison between outdoor temperature trends of the monitored rural weather and of the urban weather calculated in the case UHI_1 or UHI_2. The trends are referred to three days for each summer month. Corresponding UHI intensities and contemporaneous wind speeds are also reported.

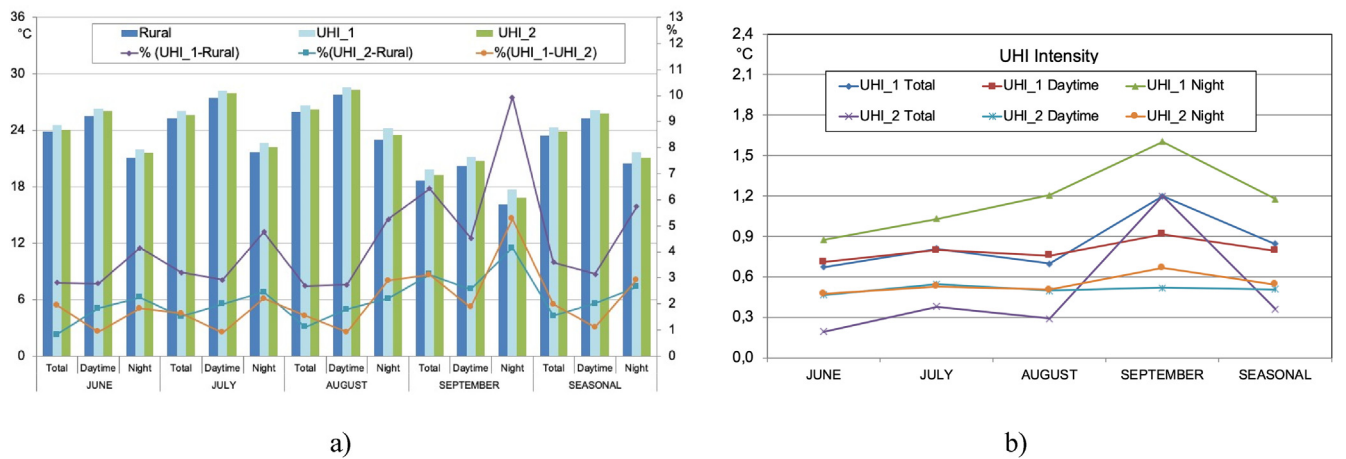


Fig. 7. Monthly and seasonal average air temperatures of the monitored rural weather and of the urban weather calculated in the case UHI_1 or UHI_2 and their percentage differences (a). The corresponding UHI intensities are reported in (b).

the urban network and seawater loop. In all the summer months, the comparison highlights the best performances of SWCCs owing to the more favorable thermal levels of the sea than outside air. Advantage accentuated in the urban area by UHI effect influencing only in the case of ACCs. The careful pumping control permits to limit the seasonal EER reduction due to pumping electric absorption only from 4.56 to 4.37 in front of a seasonal average ACC EER of 3.57. Seasonal electric energy consumption calculated for ACCs is 2.8 GWh. Owing to less cooling demand and better EER, the seasonal electric consumption is reduced to 2.14 GWh for SWCCs. The seasonal energy saving reaches 23.5%.

Chiller performance assessment in dynamic conditions provided also the trends of the thermal power dissipated by condensers and removed in different ways with the two chiller technologies. In Fig. 9b the total heat released to urban outside air from ACCs as well as the total

heat transferred away from the city in the case of SWCCs are reported in terms of monthly and seasonal average specific power per urban unit area. The less heat amount to be removed by SWCCs with respect to ACCs wasted heat is caused by the less cooling demand and better EER. The high values confirm their importance in the energy balances of the UHI in the case of ACCs and the benefit obtained thanks to SWCC technology.

In addition, Fig. 9b shows the further advantage consisting in a net reduction of the trend of CO₂ emission caused by the electric consumption due to air conditioning in urban area. Therefore, adopting the proposed technology can foster the urban actions to cut the Greenhouse Gas footprint which includes not only the direct emission from urban activities but also upstream emissions to produce goods and services for urban consumers.

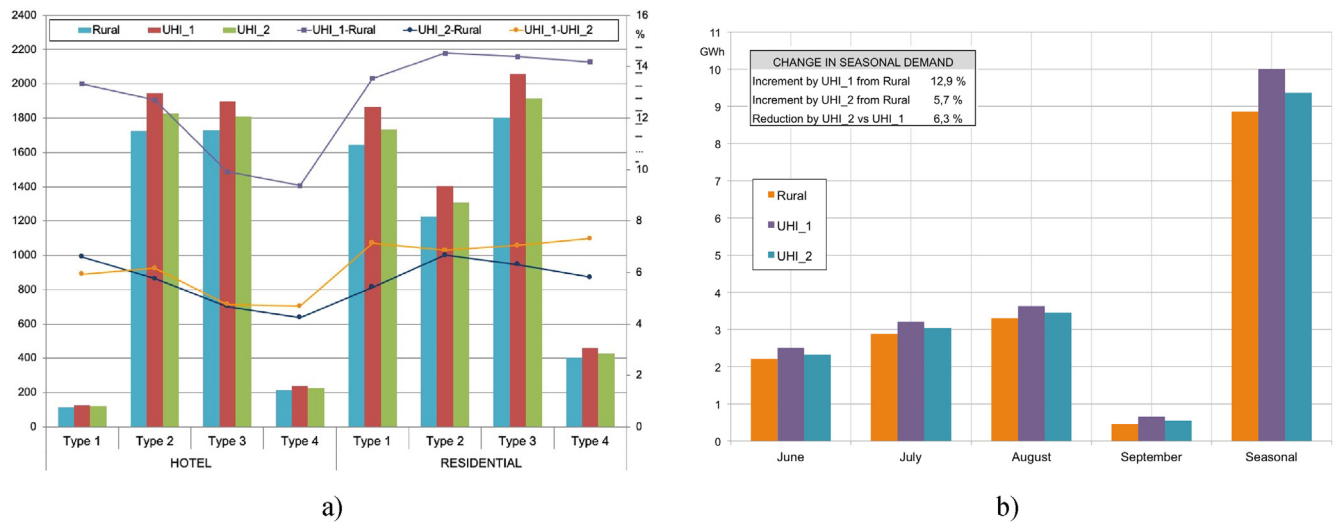


Fig. 8. Change in cooling demand with the monitored rural weather and with the calculated UHI_1 or UHI_2: total contribution of each archetype and corresponding percentage differences (a), monthly and seasonal total demands of the area and corresponding seasonal percentage changes (b).

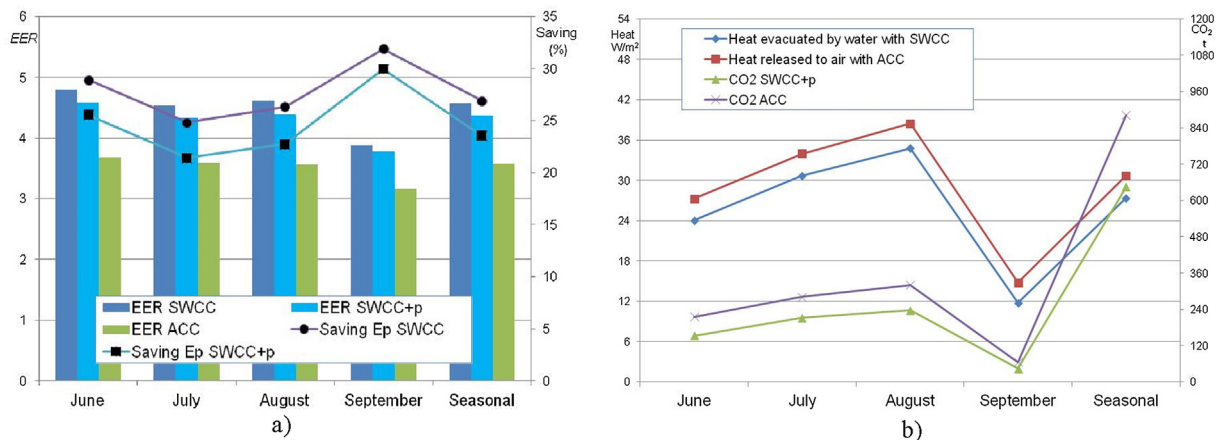


Fig. 9. Monthly and seasonal chiller performances: EER of SWCC and ACC and primary energy (Ep) savings by SWCC considering also the pumping (SWCC + p) (a). Specific thermal power evacuated by water or released to air per urban unit area and CO₂ emissions in tons corresponding to the electric absorptions of the two chillers SWCC and ACC (b).

4. Conclusion

The investigation focused about the consequences on UHI of the systematic use of air conditioning systems in urban area. An aspect often less considered than other urban and architectural features. In particular, the UHI worsening caused by the heat released by air conditioning systems in the surroundings of buildings was highlighted by referring to a precise assessment in a case study. A technical solution was proposed based on the realization of an urban cooling network able to carry away from the city the heat dissipated by chiller condensers. In presence of surface or ground water availability, water can be used as final heat sink. The UHI mitigation thus achieved is accompanied by a significant energy saving and GHG emission reduction. Indeed, the benefits of such a grid can be extended to the winter period considering the worldwide increasing diffusion of reversible heat pumps not only for air conditioning, but also for heating when required. In this event, the exploitation of renewable energy from the water as cold source is combined with the improving of the efficiency with reference to air source heat pumps or boilers. The current negative forecast suggests a reinforcement of the benefits in the next future climate change scenario. This mitigation option can be also a valid support in presence of extreme events such as heat waves and therefore it is capable to contribute to increase urban resilience.

Declaration of Competing Interest

The authors declared that there is no conflict of interest.

Appendix A. Supplementary material

Supplementary data to this article can be found online at <https://doi.org/10.1016/j.applthermaleng.2020.115390>.

References

- [1] T.F. Stocker, D. Qin, G.K. Plattner, M.M.B. Tignor, S.K. Allen, J. Boschung et al., Climate change 2013 the physical science basis: Working Group I contribution to the fifth assessment report of the intergovernmental panel on climate change, 2013. <https://doi.org/10.1017/CBO9781107415324>.
- [2] P.J.G. Ribeiro, L.A. Pena Jardim Gonçalves, Urban resilience: A conceptual framework. *Sustain Cities Soc.* 50 (2019) 101625. <https://doi.org/10.1016/j.scs.2019.101625>.
- [3] P. Marana, C. Eden, H. Eriksson, C. Grimes, J. Hernantes, S. Howick, et al., Towards a resilience management guideline — cities as a starting point for societal resilience, *Sustain Cities Soc.* (2019), <https://doi.org/10.1016/j.scs.2019.101531>.
- [4] K.K. Roman, T. O'Brien, J.B. Alvey, O.J. Woo, Simulating the effects of cool roof and PCM (phase change materials) based roof to mitigate UHI (urban heat island) in prominent US cities, *Energy* (2016), <https://doi.org/10.1016/j.energy.2015.11.082>.
- [5] M. Santamouris, Heat island research in Europe: The state of the art, *Adv. Build.*

- Energy Res. (2007), <https://doi.org/10.1080/17512549.2007.9687272>.
- [6] G. Manoli, S. Fatichi, M. Schläpfer, K. Yu, T.W. Crowther, N. Meili, et al., Magnitude of urban heat islands largely explained by climate and population, *Nature* (2019), <https://doi.org/10.1038/s41586-019-1512-9>.
- [7] X. Li, Y. Zhou, S. Yu, G. Jia, H. Li, W. Li, Urban heat island impacts on building energy consumption: A review of approaches and findings, *Energy* (2019), <https://doi.org/10.1016/j.energy.2019.02.183>.
- [8] L. Shi, Z. Luo, W. Matthews, Z. Wang, Y. Li, J. Liu, Impacts of urban microclimate on summertime sensible and latent energy demand for cooling in residential buildings of Hong Kong, *Energy* (2019), <https://doi.org/10.1016/j.energy.2019.116208>.
- [9] S. Duan, Z. Luo, X. Yang, Y. Li, The impact of building operations on urban heat/cold islands under urban densification: A comparison between naturally-ventilated and air-conditioned buildings, *Appl. Energy* (2019), <https://doi.org/10.1016/j.apenergy.2018.10.108>.
- [10] U.S. Environmental Protection Agency. Heat islands impacts, 2020. <https://www.epa.gov/heat-islands/heat-island-impacts#emissions>.
- [11] H. Akbari, Potentials of urban heat island mitigation, *Passiv. Low Energy Cool Built Environ.*, 2005.
- [12] H. Li, F. Meier, X. Lee, T. Chakraborty, J. Liu, M. Schaap, et al., Interaction between urban heat island and urban pollution island during summer in Berlin, *Sci. Total Environ.* (2018), <https://doi.org/10.1016/j.scitotenv.2018.04.254>.
- [13] H. Li, S. Sodoudi, J. Liu, W. Tao, Temporal variation of urban aerosol pollution island and its relationship with urban heat island, *Atmos. Res.* 241 (2020) 104957 <https://doi.org/https://doi.org/10.1016/j.atmosres.2020.104957>.
- [14] J. Chen, H. Wang, H. Zhu, Analytical approach for evaluating temperature field of thermal modified asphalt pavement and urban heat island effect, *Appl. Therm. Eng.* 113 (2017) 739–748 <https://doi.org/https://doi.org/10.1016/j.appltherm-eng.2016.11.080>.
- [15] J.Y. Deng, N.H. Wong, Impact of urban canyon geometries on outdoor thermal comfort in central business districts, *Sustain Cities Soc.* (2020), <https://doi.org/10.1016/j.scs.2019.101966>.
- [16] D.J. Sailor, M. Georgescu, J.M. Milne, M.A. Hart, Development of a national anthropogenic heating database with an extrapolation for international cities, *Atmos. Environ.* (2015), <https://doi.org/10.1016/j.atmosenv.2015.07.016>.
- [17] B. Castellani, E. Morini, E. Anderini, M. Filippini, F. Rossi, Development and characterization of retro-reflective colored tiles for advanced building skins, *Energy Build.* (2017), <https://doi.org/10.1016/j.enbuild.2017.08.078>.
- [18] E. Morini, B. Castellani, A. Presciutti, E. Anderini, M. Filippini, A. Nicolini, et al., Experimental analysis of the effect of geometry and façade materials on urban district's equivalent albedo, *Sustain* (2017), <https://doi.org/10.3390/su9071245>.
- [19] F. Bisegna, A. Buggin, G. Peri, G. Rizzo, G. Scaccianoce, M. Scarpa et al., Computing methods for resilience: Evaluating new building components in the frame of SECAPs, in: *Proc. - 2019 IEEE Int. Conf. Environ. Electr. Eng. 2019 IEEE Ind. Commer. Power Syst. Eur. EEEIC/I CPS Eur.* 2019, 2019. <https://doi.org/10.1109/EEEIC.2019.8783458>.
- [20] P. Bevilacqua, R. Bruno, N. Arcuri, Green roofs in a Mediterranean climate: energy performances based on in-situ experimental data, *Renew. Energy* (2020), <https://doi.org/10.1016/j.renene.2020.01.085>.
- [21] F. Aram, E. Higuera García, E. Solgi, S. Mansournia, Urban green space cooling effect in cities, e01339–e01339, *Heliyon* 5 (2019), <https://doi.org/10.1016/j.heliyon.2019.e01339>.
- [22] D.J. Sailor, H. Fan, The importance of including anthropogenic heating in mesoscale modeling of the urban heat island, *Bull. Am. Meteorol. Soc.* (2004).
- [23] C. Smith, S. Lindley, G. Levermore, Estimating spatial and temporal patterns of urban anthropogenic heat fluxes for UK cities: The case of Manchester, *Theor. Appl. Climatol.* (2009), <https://doi.org/10.1007/s00704-008-0086-5>.
- [24] Y. Cui, D. Yan, T. Hong, J. Ma, Temporal and spatial characteristics of the urban heat island in Beijing and the impact on building design and energy performance, *Energy* (2017), <https://doi.org/10.1016/j.energy.2017.04.053>.
- [25] R. Sun, Y. Wang, L. Chen, A distributed model for quantifying temporal-spatial patterns of anthropogenic heat based on energy consumption, *J. Clean. Prod.* (2018), <https://doi.org/10.1016/j.jclepro.2017.09.153>.
- [26] Y. Wen, Z. Lian, Influence of air conditioners utilization on urban thermal environment, *Appl. Therm. Eng.* (2009), <https://doi.org/10.1016/j.applthermaleng.2008.03.039>.
- [27] V.Q. Doan, H. Kusaka, T.M. Nguyen, Roles of past, present, and future land use and anthropogenic heat release changes on urban heat island effects in Hanoi, Vietnam: Numerical experiments with a regional climate model, *Sustain Cities Soc.* (2019), <https://doi.org/10.1016/j.scs.2019.101479>.
- [28] C. Guattari, L. Evangelisti, C.A. Balaras, On the assessment of urban heat island phenomenon and its effects on building energy performance: A case study of Rome (Italy), *Energy Build.* (2018), <https://doi.org/10.1016/j.enbuild.2017.10.050>.
- [29] X. Yang, L. Yao, L.L.H. Peng, Z. Jiang, T. Jin, L. Zhao, Evaluation of a diagnostic equation for the daily maximum urban heat island intensity and its application to building energy simulations, *Energy Build.* (2019), <https://doi.org/10.1016/j.enbuild.2019.04.001>.
- [30] X. Yang, L.L.H. Peng, Z. Jiang, Y. Chen, L. Yao, Y. He, et al., Impact of urban heat island on energy demand in buildings: Local climate zones in Nanjing, *Appl. Energy* (2020), <https://doi.org/10.1016/j.apenergy.2019.114279>.
- [31] N. Lauzet, A. Rodler, M. Musy, M.H. Azam, S. Guernouti, D. Mauree, et al., How building energy models take the local climate into account in an urban context – A review, *Renew. Sustain. Energy Rev.* (2019), <https://doi.org/10.1016/j.rser.2019.109390>.
- [32] M. Palme, L. Inostroza, G. Villacreses, A. Lobato-Cordero, C. Carrasco, From urban climate to energy consumption. Enhancing building performance simulation by including the urban heat island effect, *Energy Build.* (2017), <https://doi.org/10.1016/j.enbuild.2017.03.069>.
- [33] B. Bueno, L. Norford, J. Hidalgo, G. Pigeon, The urban weather generator, *J. Build. Perform. Simul.* (2013), <https://doi.org/10.1080/19401493.2012.718797>.
- [34] U.S. Department of Energy. EnergyPlus, 2019, n.d. <https://energyplus.net>.
- [35] A. Salvati, M. Palme, L. Inostroza, Key parameters for urban heat island assessment in a mediterranean context: a sensitivity analysis using the urban weather generator model, *IOP Conf. Ser. Mater. Sci. Eng.* (2017), <https://doi.org/10.1088/1757-899X/245/8/082055>.
- [36] I. Sarbu, C. Sebarchievici, General review of ground-source heat pump systems for heating and cooling of buildings, *Energy Build.* (2014), <https://doi.org/10.1016/j.enbuild.2013.11.068>.
- [37] L. Schibuola, C. Tambani, A. Zarrella, M. Scarpa, Ground source heat pump performance in case of high humidity soil and yearly balanced heat transfer, *Energy Convers. Manag.* 76 (2013) 956–970, <https://doi.org/10.1016/j.enconman.2013.09.002>.
- [38] Z. Luo, C. Asproudi, Subsurface urban heat island and its effects on horizontal ground-source heat pump potential under climate change, *Appl. Therm. Eng.* (2015), <https://doi.org/10.1016/j.applthermaleng.2015.07.025>.
- [39] J. Liang, Q. Yang, L. Liu, X. Li, Modeling and performance evaluation of shallow ground water heat pumps in Beijing plain, China, *Energy Build.* (2011), <https://doi.org/10.1016/j.enbuild.2011.08.007>.
- [40] Y. Nam, R. Ooka, Numerical simulation of ground heat and water transfer for groundwater heat pump system based on real-scale experiment, *Energy Build.* (2010), <https://doi.org/10.1016/j.enbuild.2009.07.012>.
- [41] L. Schibuola, C. Tambani, Renewable energy sources for historic buildings: The Crucifers convent in Venice, *WIT Trans. Ecol. Environ.* (2012) 165, <https://doi.org/10.2495/ARC120301>.
- [42] X. Chen, G. Zhang, J. Peng, X. Lin, T. Liu, The performance of an open-loop lake water heat pump system in south China, *Appl. Therm. Eng.* (2006), <https://doi.org/10.1016/j.applthermaleng.2006.03.009>.
- [43] Y. Hak Song, Y. Akashi, J.J. Yee, Effects of utilizing seawater as a cooling source system in a commercial complex, *Energy Build.* (2007). <https://doi.org/10.1016/j.enbuild.2006.11.011>.
- [44] X. li Li, L. Duanmu, H. wen Shu, Optimal design of district heating and cooling pipe network of seawater-source heat pump, *Energy Build.* (2010). <https://doi.org/10.1016/j.enbuild.2009.07.016>.
- [45] Y.J. Baik, M. Kim, K.C. Chang, Y.S. Lee, H.S. Ra, Potential to enhance performance of seawater-source heat pump by series operation, *Renew. Energy* (2014), <https://doi.org/10.1016/j.renene.2013.09.021>.
- [46] U.S. Department of Energy. EnergyPlus Version 9.2.0, Documentation- Auxiliary Programs. Sept 27, 2019, n.d. https://energyplus.net/sites/all/modules/custom/nrel_custom/pdfs/pdfs_v9.2.0/AuxiliaryPrograms.pdf.
- [47] L.G. Swan, V.I. Ugursal, Modeling of end-use energy consumption in the residential sector: A review of modeling techniques, *Renew. Sustain. Energy Rev.* (2009), <https://doi.org/10.1016/j.rser.2008.09.033>.
- [48] A. Nakano, B. Bueno, L.Norford, C.F. Reinhart, Urban weather generator - A novel workflow for integrating urban heat island effect within urban design process, in: *14th Int. Conf. IBPSA - Build. Simul. 2015, BS 2015, Conf. Proc.*, 2015.
- [49] MIT. Urban Weather Generator, 2014. <http://urbanmicroclimate.scripts.mit.edu/uwg.php>.
- [50] L. Schibuola, M. Scarpa, Ground source heat pumps in high humidity soils: An experimental analysis, *Appl. Therm. Eng.* 99 (2016) 80–91, <https://doi.org/10.1016/j.applthermaleng.2016.01.040>.
- [51] National Law. Provisions on the protection of the waters from pollution "Disposizioni sulla tutela delle acque dall'inquinamento", *Dlgs.n.152, 11 May 1999*, Italy n.d.
- [52] L. Schibuola, M. Scarpa, C. Tambani, Innovative technologies for energy retrofit of historic buildings: An experimental validation, *J. Cult. Herit.* (2017), <https://doi.org/10.1016/J.CULHER.2017.09.011>.
- [53] RHOSS. TCHEY-THHEY 245÷2187, Y-flow low consumption range, technical bulletin K20325EN ed.11. 2019.
- [54] CEN. EN 14511-3:2019 Air conditioners, liquid chilling packages and heat pumps for space heating and cooling and process chillers, with electrically driven compressors (Parts 3: Test methods). 2019.
- [55] S. Marinhas, Eurovent chiller certification key stones and future challenges, *REHVA J.* (2013) 31–33.
- [56] L. Schibuola, M. Scarpa, C. Tambani, Modelling of HVAC system components for building dynamic simulation, in: *Proc. BS 2013 13th Conf. Int. Build. Perform. Simul. Assoc.*, 2013.
- [57] CEN. EN 14825:2018 Air conditioners, liquid chilling packages and heat pumps, with electrically driven, compressors, for space heating and cooling - Testing and rating at part load conditions and calculation of seasonal performance 2018:139.